



Targeting the PANoptosome Using Necrostatin-1 Reduces PANoptosis and Protects the Kidney Against Ischemia-Reperfusion Injury in a Rat Model of Controlled Experimental Nonheart-Beating Donor

Mehmet Dokur^{a*}, Erdal Uysal^b, Faruk Kucukdurmaz^c, Serdar Altınay^d, Sait Polat^e, Kadir Batcioglu^f, Yakup Yilmaztekin^f, Turkan Guney^g, Tugce Sapmaz Ercakalli^e, Asli Yaylali^h, Efe Sezginⁱ, Zafer Cetin^j, Eyup Ilker Saygili^k, Osman Barut^l, Hatem Kazimoglu^m, Gokturk Maralcan^b, Suna Kocⁿ, Mehmet Sokucu^o, and Sema Nur Dokur Yeni^p

^aDepartment of Emergency Medicine, Biruni University Faculty of Medicine, Istanbul, Turkey; ^bDepartment of General Surgery, Sanko University Faculty of Medicine, Gaziantep, Turkey; ^cDepartment of Urology, Defa Life Hospital, Gaziantep, Turkey; ^dDepartment of Pathology, University of Health Sciences Faculty of Medicine, Antalya City Hospital, Antalya, Turkey; ^eDepartment of Histology and Embryology, Cukurova University Faculty of Medicine, Adana, Turkey; ^fDepartment of Biochemistry, Inonu University Faculty of Pharmacy, Malatya, Turkey; ^gDepartment of Medical Biochemistry, Bilecik Şeyh Edebali University Faculty of Medicine, Bilecik, Turkey; ^hDepartment of Histology and Embryology and IVF Center, Kahramanmaraş Sutcu Imam University Faculty of Medicine, Kahramanmaraş, Turkey; ⁱDepartment of Food Engineering, Izmir Institute of Technology, Izmir, Turkey; ^jDepartment of Medical Biology, Sanko University Faculty of Medicine, Gaziantep, Turkey; ^kDepartment of Medical Biochemistry, Sanko University Faculty of Medicine, Gaziantep, Turkey; ^lDepartment of Urology, Kahramanmaraş Sutcu Imam University Faculty of Medicine, Kahramanmaraş, Turkey; ^mDepartment of Urology, Sanko University School of Medicine, Gaziantep, Turkey; ⁿDepartment of Anesthesiology and Reanimation, Biruni University Faculty of Medicine, Istanbul, Turkey; ^oDepartment of Pathology, Sanko University Faculty of Medicine, Gaziantep, Turkey; and ^pDepartment of Internal Medicine, Marmara University Faculty of Medicine, Istanbul, Turkey

ABSTRACT

Purpose. Reducing renal ischemia is crucial for the function and survival of grafts from non-heartbeat donors, as it leads to inflammatory responses and tubulointerstitial damage. The primary concern with organs from nonheartbeat donors is the long warm ischemia period and reperfusion injury following renal transplantation. This study had two main goals; one goal is to determine how Necrostatin-1 targeting the PANoptosome affects PANoptosis in the nonheart-beating donor rat model. The other goal is to find out if Necrostatin-1 can protect the kidney from ischemic injury for renal transplantation surgery.

Methods. Twenty-four rats were grouped randomly as control and Necrostatin-1 in this experimental animal study, and we administered 1.65 mg/kg of Necrostatin-1 intraperitoneally to the experimental group for 30 minutes before cardiac arrest. We removed the rats' left kidneys and measured various oxidative stress marker measures such as malondialdehyde, superoxide dismutase, catalase, GPx, and 8-hydroxy-2-deoxyguanosine levels. We then subjected the tissues to immunohistochemical analysis, electron microscopy, and histopathological analysis.

Findings. The Necrostatin-1 group had a lower total tubular injury score ($P < .001$) and less Caspase-3, gasdermin D, and mixed lineage kinase domain-like protein expression. Additionally, the apoptotic index of the study group was lower ($P < .001$). Furthermore, the study group had higher levels of superoxide dismutase and GPx ($P < .05$), whereas malondialdehyde levels were reduced ($P = .009$). Electron microscopy also revealed a significant improvement in tissue structure in the Necrostatin-1 group.

*Address correspondence to: Dokur Mehmet, Department of Emergency Medicine, Biruni University Faculty of Medicine, Gultepe Mah. Halkalç Cad. No: 99, 34295 Kucukcekmece, Istanbul, Turkey. E-mail: drdokur@gmail.com

Conclusion. Necrostatin-1 protects against ischemic acute kidney injury in nonheart-beating donor rats by inhibiting PANoptosis via the blockade of RIPK1. As a result of this, Necrostatin-1 may offer novel opportunities for protecting donor kidneys from renal ischemia-reperfusion injury during transplantation in patients with end-stage kidney disease requiring a renal transplantation.

RENAL transplantation is the gold standard to treat end-stage kidney disease, but the number of patients in need of an organ exceeds the number of available donors. In recent years, donors after circulatory death (DCD) or nonheart-beating donors (NHBDs) have been used to increase the donor pool, as the number of brain-dead donors has not risen to meet the demand [1]. The introduction of NHBD in kidney and liver transplantation has increased the donor pool by approximately 20%. The overall 5-year patient and graft survival rates were 80% to 90% and 72% to 86% of renal transplantation donors with cadaveric or NHBDs, respectively [2,3]. But in NHBD, prolonged warm ischemia time (WIT) leads to inflammation, cell damage, and tubular injury. This is why reducing the damage from renal ischemia is so important for graft function and survival [4]. The primary concern with organs from NHBD is the long warm ischemia period and reperfusion injury following renal transplantation. Renal ischemia-reperfusion injury (RIRI) often leads to delayed graft function (DGF) and graft loss, which has been linked to more death and illness [5]. The complex pathophysiology of RIRI is a result of pyroptosis, which exacerbates structural and functional kidney damage, as well as apoptosis and necroptosis in the renal tubular epithelium [6]. The essential process of necroptosis involves the activation, including ubiquitination and phosphorylation, of receptor-interacting protein 1 (RIP1 or RIPK1) or, receptor-interacting protein 3 (RIP3 or RIPK3), and mixed lineage kinase domain-like protein (MLKL) [7]. Recent studies have also connected necroptosis, another form of programmed cell death, to renal ischemia. Therefore, restricting or minimizing the effects of pyroptosis, apoptosis, and necroptosis might offer robust protection against RIRI. It has only recently been discovered that apoptosis (A), necroptosis (N), and pyroptosis (P) may all be regulated in concert to create a novel route of programmed cell death known as PANoptosis [8,9]. The protein complex PANoptosome, located in the cytoplasm, controls this pathway and triggers the three distinct forms of programmed cell death it controls [9]. Before the discovery of PANoptosis, it was believed that these three pathways functioned independently of one another [10]. The role of PANoptosis in diseases and the potential implications of PANoptosis in cancer prognosis and immunotherapy are among the trending topics of research [11,12]. Based on this relationship, it seems that preventing PANoptosis—which includes apoptosis, mitoptosis, necrosis, necroptosis, autophagy, mitophagy, mitochondrial permeability transition-driven necrosis, ferroptosis, pyroptosis, cuproptosis, and parthanoptosis—by focusing on a protein of the PANoptosome could be important for reducing the damage that ischemia does to the kidneys [7]. Nec-1 or methyl-thiohydantoin-tryptophan is a low molecular

weight alkaloid recognized as an inhibitor of RIP1 and indoleamine 2,3-dioxygenase. Nec-1 interrupts the necroptosis signaling pathways by obstructing RIP1 signaling cascades. Moreover, Nec-1 influences necroptosis via modulating reactive oxygen species (ROS). Nec-1 mitigates apoptosis by targeting RIP1 during the RIP1-dependent apoptosis signaling route, while this anti-apoptotic impact is diminished in the RIP1-independent apoptosis pathway. Nec-1 inhibits RIP1 kinase activity and afterward, RIP1 autophosphorylation even more strongly. This is an important step in the signaling process for tumor necrosis factor-induced necroptosis. RIP1 phosphorylation facilitates RIP1 and RIP3 complex formation. Following the phosphorylation and oligomerization of MLKL, Complex IIc forms, signaling the onset of necroptosis. In summary, Nec-1 effectively hinders RIP1-RIP3-MLKL signaling by preventing RIP1 phosphorylation, and it also reduces renal ischaemia-reperfusion damage (time-dependent) by inhibiting the RIP1-induced inflammatory immune response. Nec-1, which is effective on multiple processes such as apoptosis and necroptosis, protects renal tubular epithelial cells in acute kidney damage, mitigates necroptotic cell death, and improves kidney function; it also lowers blood creatinine and urea concentrations in RIRI rat models [13,14].

In this study, we demonstrated the nephroprotective effect of Nec-1 in a NHBD rats by using histopathological, immunohistochemical, and electromicroscopic methods to show how it reduces necroptotic cell death in the renal tubular epithelium after acute ischemia. Besides, we observed changes in ROS levels in the ischemic tubulo-interstitial renal tissue during this process. In fact, we targeted to prove whether Nec-1 is a useful nephroprotective agent in renal transplantation practices through a donor rat model.

MATERIALS AND METHODS

Study Population

We included 24 female Wistar Albino rats in this study and randomly divided them into two groups: the control group (Group 1, $n = 12$) and the experimental, or Nec-1, group (Group 2, $n = 12$). The age range was 10 to 12 weeks, and the weight range was 200 to 250 g. This experimental animal study was conducted in accordance with the principles of “Directive 2010/63/EU of the European Parliament and of the Council of September 22, 2010, on the protection of animals (performing surgical procedures under anesthesia to ensure animal welfare and to avoid pain, suffering, and discomfort) used for scientific purposes” (Text with EEA relevance, Document 02010L0063-20190626). Approval for the conduct of this study was obtained from the Institutional Animal Ethics Committee of

Kahramanmaraş Sutcu Imam University (decision date: June 16, 2021, and decision number: 04, Kahramanmaraş, Turkey).

Environment of Experimental Animals and Creating a Rat Model of Controlled Experimental NHBD

In a conventional experimental animal laboratory environment at Kahramanmaraş Sutcu Imam University (Turkey) with a temperature range of 18 to 24°C and a light-dark cycle of 12 hours, the rats had unrestricted access to food and water. Rats in group 1 received 1.25 mL of saline with 1% dimethyl sulfoxide intraperitoneally 30 minutes before cardiac arrest. Group 2 rats administered Nec-1.65 mg/kg, body weight in a total volume of 200 µL (Sigma Aldrich, Saint-Louis, Missouri, USA) diluted in 1.25 mL of saline with 1% dimethyl sulfoxide before cardiac arrest with potassium chloride (KCL) in the NBHD rat model [13,15]. We considered the relatively short half-life of Nec-1 and its use earlier than the onset of ischemic injury in the kidney, defining the timing for Nec-1 administration. Also, we determined the dosing of Nec-1 for this study in the current research based on the doses used in the experimental rat study by Linkermann et al, which evaluated the role of RIP1 in mediating necroptosis and its effect on RIRI [17]. We administered combined ketamine (75 mg/kg) (Ketalar, Pfizer, Turkey) and xylazine (10 mg/kg) (Rompun, Bayer AG, Leverkusen, Germany) intraperitoneally for anesthesia. We induced cardiac arrest by directly infusing potassium chloride (KCl) into the heart, a method commonly used for NHBD models [16]. We chose this method due to its effectiveness in creating an NHBD simulation and its ease of administration. We specifically infused 2 mmol/kg (0.9 mmol/lb) of potassium chloride intracardiacally under anesthesia [17]. We performed a standard ipsilateral nephrectomy through a midline abdominal incision after 60 minutes of cardiac arrest. In this NHBD rat model, we defined the optimal duration of ischemic injury as the initial period of WIT following the determination of circulatory death. Current literature on transplant surgery indicates that maintaining warm ischemia duration below 30 minutes is essential for optimal graft function, while durations exceeding 50 minutes following renal transplantation are considered unfavorable. To determine the optimal timing for ischemic injury, we considered the brief half-life of Nec-1, which is 1 to 2 hours (1.8 ± 0.9) [18,19], alongside the onset of ischemic injury during WIT or nonheart-beating time in this controlled NHBD rats. In addition, our previous experimental study, which demonstrated the healing effect of milrinone on RIRI in the controlled NHBD donor rat model, also assisted us in determining the optimal ischemic injury duration [20]. We divided the resected renal tissue into three equal parts. The first part was placed in an Eppendorf test tube and stored at -80°C for biochemical analysis. We preserved the second part for electron microscopic evaluation in a 5% glutaraldehyde solution. We reserved the third part for histopathological and immunohistochemical examination in formalin solution.

Histopathological Processing, Evaluation, and Grading

We fixed the rat kidney samples in a 10% buffered formaldehyde solution and sent them for pathological examination. We

kept the renal samples in the same solution for 2 days before the examination and then embedded them in paraffin. We cut and stained 4 mm-thick slices with hematoxylin and eosin. We evaluated the histopathological changes under a light microscope (Nikon Ni 50, Japan). A board-certified pathologist examined the extent of kidney damage histopathologically, blinded to the experimental groups. We graded each sample using a previously described scoring system (range: 0-4) [20].

Immunohistochemical Assessment

We performed the immunohistochemical analysis using a Ventana Medical Systems device (Roche Tissue Diagnostics, Arizona, USA). The antibodies used for staining were MKLK (Mouse Mab#3B2, clone no. 293201, 1/1000 dilution, Santa Cruz Biotechnology Inc., Santa Cruz, California, USA), Gasdermin Cleaved Gasdermin D (Rabbit Mab#36425, clone no. Asp275, E7H9G, 1/1500 dilution, Cell Marq, USA), and Caspase-3 Cleaved Caspase-3 (Rabbit Mab#9661, clone no. Asp175, 1/1400 dilution, Cell Marq, USA). We followed the manufacturer's instructions after xylene deparaffinization.

Caspase-3 Evaluation

We used the standard avidin-biotin-peroxidase complex method for immunohistochemical analysis to measure caspase-3 levels [21]. We mixed it with a polyclonal Caspase-3 antibody (Ventana Medical Systems, Roche Tissue Diagnostics, Arizona, USA) until it was 1:100, and then used an avidin-biotin HRP procedure to color the sections. We performed a total of 22 Caspase-3 measurements on the tissue samples.

We calculated the apoptotic index using the formula below:

$$\frac{\text{the average number of cells that are Caspase - 3 plus from five random fields}}{\text{The average number of total cells in 5 different fields}} \times 100$$

The Study Evaluated Gasdermin D (GSDMD-N) and MLKL (Mixed-Lineage Kinase Domain-Like)

We semiquantitatively evaluated the immunohistochemical staining distribution pattern by assigning scores. We classified the staining strength as 0 (no expression), 1+ (weak staining), 2+ (moderate staining), and 3+ (strong staining). We also scored the percentage of p53-positive cells as 0 (negative or uncommon plus cells), 1 (10% positive cells), 2 (10%-25% positive cells), 3 (26%-50% positive cells), 4 (51%-75% positive cells), or 5 (>75% positive cells). The range of 0 to 15 was the result of multiplying the staining strength and staining percentage scores.

Electron Microscopy Evaluation

After being fixed in glutaraldehyde for the first time, the kidney samples were treated again for 3 hours in a phosphate buffer solution (Millonig). We shaken the kidney samples twice in the buffer for 10 minutes before transferring them to a 1 percent osmium tetroxide solution for 2 hours. Next, using phosphate

buffer, we rinsed the tissue twice for 10 minutes. After dehydrating the samples with a series of ethyl alcohol concentrations (50, 70, 86, 96, and 100 percent) for 15 minutes each, we treated them with propylene oxide twice for 15 minutes, and then with propylene oxide + resin twice for 30 minutes each time. We placed renal tissue pieces in tubes containing mixed resin for 6 hours. We embedded the kidney tissue pieces in Beem tablets using the newly created embedding material before polymerizing them in a drying oven at 60°C for 2 days. We used the Leica Reichert Ultracut S Ultramicrotome (Austria) to make the 50 nm-thick slices. To stain the tissue slices, we prepared saturated uranyl acetate with 70% ethyl alcohol and lead citrate solutions. We used transmission electron microscopy to examine and capture images of the stained slices (Japan). For all electron microscopic tissue examinations in this study, the bar is 1 μ m.

Biochemical Analyzes

We determined protein concentrations using the Bradford method [22]. We assessed the levels of malondialdehyde (MDA) using the Mihara and Uchiyama method [23] and determined the efficiency of superoxide dismutase (SOD) using Joe M. McCord's technique [24]. We evaluated catalase (CAT) activity using the Luck [25] protocol, and measured glutathione peroxidase (GPx) activity using Lawrence RA's method [26]. We used the LCMSM technique, as previously described by Gupta [27], to determine the level of 8-hydroxy-2-deoxyguanosine (8-OHdG) and measured it spectrophotometrically. We used the Agilent Technologies 1200 series G6460C triple quadrupole HPLC/MS/MS with Jet-StreamW (ESI-MS/MS; Agilent, USA) LC-MS/MS system for the instrumental analysis of 8-OHdG after hydrolyzing DNA with formic acid, as previously described [28,29]. In addition, 50% acetonitrile and 50% 5 mM ammonium acetate in 0.1% acetic acid in water made up the mobile phase. We reported the 8-OHdG levels in nanograms per milligram of DNA.

Statistical Analysis

We used the Shapiro–Wilk and Ansari-Bradley tests to test the normality and homogeneity of variances. We used the Welch two-sample test to identify differences between the control and experimental groups if the variables had a normal distribution. We used the nonparametric Wilcoxon test if the variables did not follow a normal distribution. We used Open-access R software, Version 3.6.1 (R Foundation for Statistical Computing, Vienna, Austria), for statistical analyses.

RESULTS

Histopathologic Evaluation of Tubular Injury

Based on the histopathological scoring, the Nec-1 group had a lower degree of renal damage than the control group (see Fig 1). In the control group, 8 rats had moderate renal damage (score 3) and 4 rats had severe damage (score 4), with a mean score of 3.3 ± 0.5 . In contrast, only 2 rats in the Nec-1 group

had no kidney damage (score 0), while 5 rats had minimally severe damage (score 1) and 5 rats had mild damage (score 2), with a mean score of 1.3 ± 0.8 . The difference in mean scores between the two groups was statistically significant ($P = .016$) (see Table 1).

Immunohistochemical Assessment

Caspase-3 Expression. An immunohistochemical analysis showed that the control group had more Caspase-3, a protein that shows cells have died through apoptosis, than the Nec-1 group. In the control group, Caspase-3 staining was more prominent in all the glomerular, tubular, and interstitial areas (see Fig. 2A and 2B). The control group also had a higher apoptotic index (API), which shows the percentage of cells that have died in a sample. This was demonstrated in the glomerulus and renal tubulointerstitium (see Fig 3A and 3B). In the control group, the API range, mean, and standard deviation for tubules, interstitium, and the kidney were 16 to 24 (19.8 ± 2.2). In the Nec-1 group, the API range, mean, and standard deviation for kidney tubules were 3 to 5 (4.3 ± 0.8) ($P < .001$) (see Table 1).

Gasdermin D Activation. Gasdermin D staining was more off in the control group than in the study or Nec-1 groups. Only one rat had moderate staining (scoring 2+), while 11 rats had severe staining (scoring 3+) (see Figs 2C, 2D, and 3C). A total of 83% (10/12) of stains covered 50% to 75% of the renal tissue, resulting in a total scoring range, mean, and standard deviation values of 8 to 15 (11.7 ± 1.7). In contrast, in the Nec-1 group, two rats had no staining, and five rats had weak (scoring 1+) and mild (scoring 2+) staining. A total of 67% (8/12) of stains comprised 10% to 25% of the renal parenchyma, resulting in a total scoring range, mean, and standard deviation of 0 to 6 (2.6 ± 1.8). Gasdermin D staining was statistically higher in the control group than in the Nec-1 group ($P < .001$) (see Table 1).

MLKL Staining. We did an MLKL immunohistochemical analysis and found that the control group had a lot more MLKL staining than the Nec-1 study group (see Figs 2E, 2F, and 3D). Specifically, only two rats in the control group had moderate staining (scoring 2+), while 10 rats had severe staining (scoring 3+). In contrast, in the Nec-1 group, five rats had weak staining (score 1+) and seven rats had moderate staining (score 2+). Furthermore, the staining covered a larger proportion of the renal parenchyma in the control group (50%-75%) compared to the Nec-1 group (10%-25%). We determined the total scoring range, mean, and standard deviation to be 6 to 12 (10.2 ± 2.1) in the control group and 1 to 6 (3.3 ± 1.8) in the Nec-1 group. These findings indicate that Nec-1 treatment reduced MLKL staining and its associated cell death ($P < .05$) (see Table 1).

Electron Microscopy Results. Electron microscopy analysis showed that the proximal tubular cells in the control group were dying. This was clear because the electron density dropped, mitochondria inflated, chromatin was off, cytoplasmic bleb-like protrusions showed up, microvilli were lost, and there were more vacuoles and swollen areas. There was also more heterochromatin in the nucleus of endothelial cells in the glomerulus than in the stalks and podocytes (see Fig 4A and 4B). Nec-1,

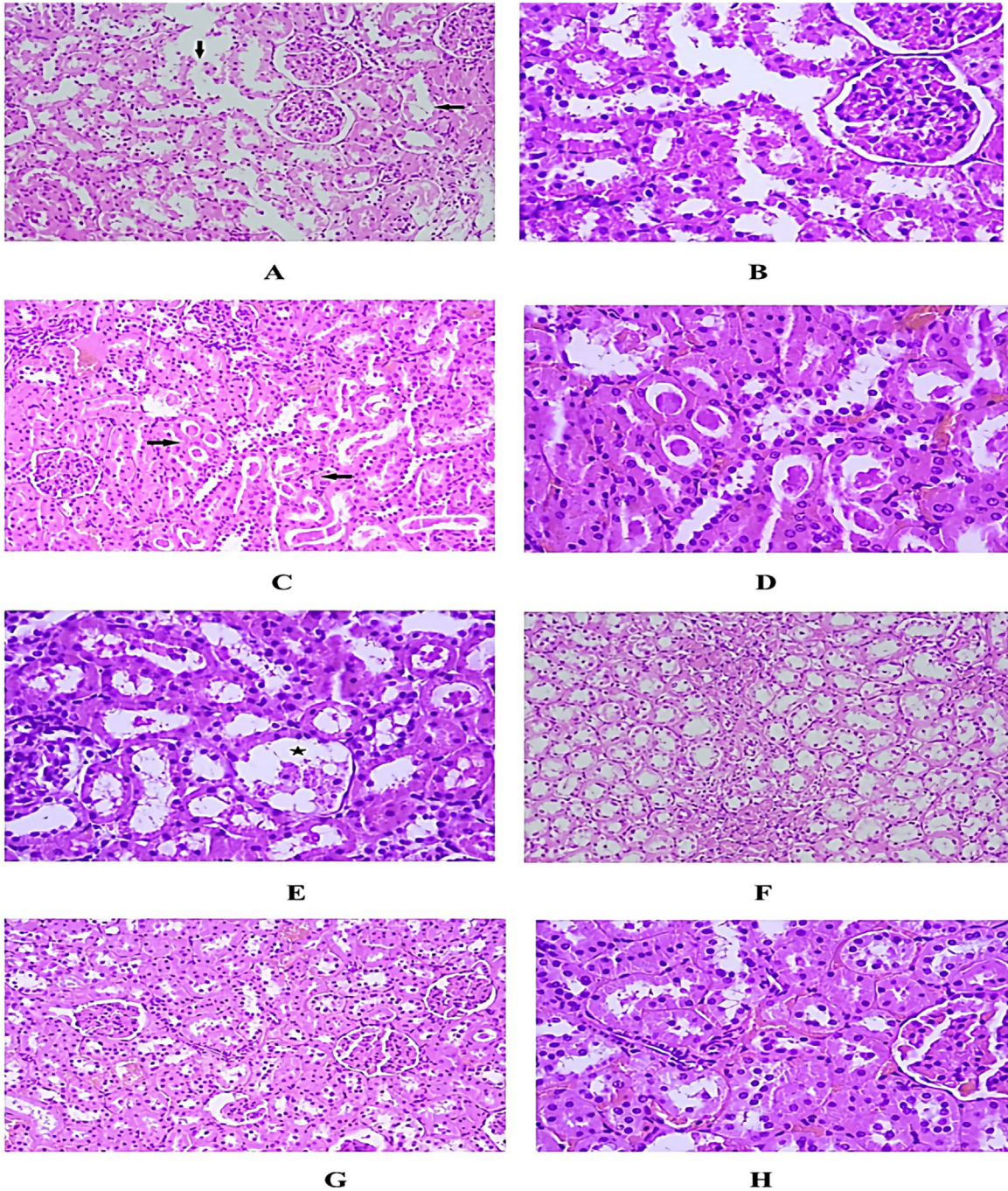


Fig 1. Histopathological examination of renal parenchymal tissue in experimental ischemic rat model. **(A)** Microscopic picture shows separation (black arrows) in the renal tubular epithelium in the control group (H&E $\times 200$). **(B)** Renal tubular injury at high magnification in the control group (H&E $\times 400$). **(C)** Eosinophilic casts are seen (arrows) in the lumens of the renal tubules in the control group (H&E $\times 200$). **(D)** Renal tubular casts at high magnification in the control group (H&E $\times 400$). **(E)** Apoptotic bodies are seen (star) in the dilated tubule lumen in the control group (H&E $\times 400$). **(F)** Interstitial nephritis findings in the control group (H&E $\times 200$). **(G)** Renal damage was significantly reduced in rats given Necrostatin-1 (H&E $\times 200$). **(H)** Renal parenchyma with almost normal morphology is observed at high magnification (H&E $\times 400$).

Table 1. Histopathological and Immunohistochemical Assessment After Renal Ischemic Injury

Ischemic Parameters	Group 1 (Control) (n = 12)	Group 2 (Nec-1) (n = 12)	P*
Tubular injury	3-4 (3.3 ± 0.5)	0-2 (1.3 ± 0.8)	.016
Apoptotic index			
<i>Glomerulus</i>	10-18 (14.2 ± 2.5)	3-6 (4.7 ± 0.9)	<.001
<i>Tubules</i>	16-24 (19.8 ± 2.2)	3-5 (4.3 ± 0.8)	<.001
Gasdermin D	8-15 (11.7 ± 1.7)	0-6 (2.6 ± 1.8)	<.001
MLKL	6-12 (10.2 ± 2.1)	1-6 (3.3 ± 1.8)	<.05

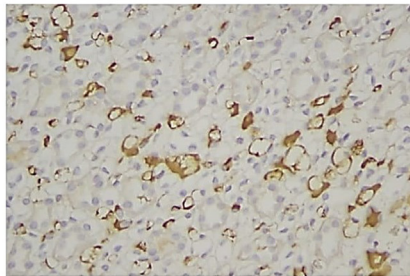
MLKL, Mixed Lineage Kinase Domain Like Pseudokinase; Nec-1, Necrostatin-1.

* P-values obtained from nonparametric Wilcoxon test.

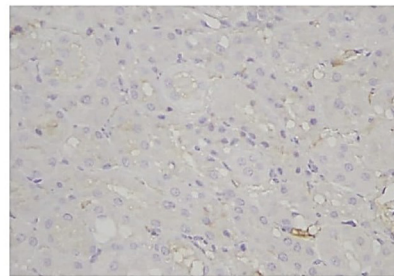
which halted necroptotic kidney cell death, improved the ultra-structural appearance of the kidneys in rats. Even though renal tubular cells had morphological problems like intracellular edema, vacuoles, and basal lamina rupture, Nec-1 made these conditions a lot better. In addition to this, the glomerulus showed normal fine structure in mesangial cells and podocytes (see Fig 4C and 4D).

Biochemical Analyzes. The results of the comparison between the two groups for SOD and GPx activity indicate that the experimental group had significantly higher activity than the controls ($P = .007$ and $P = .006$, respectively). The experimental group also showed an increase in CAT activity, although the difference between the groups was not statistically

Caspase 3

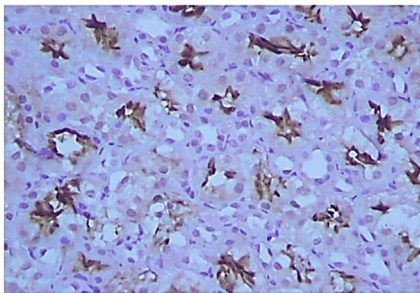


A. Control Group

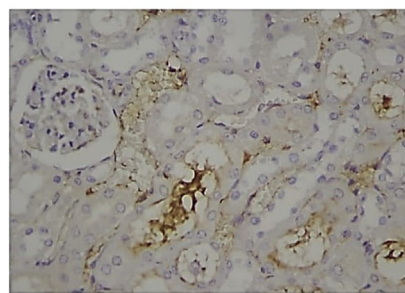


B. Necrostatin-1 Group

Gasdermin-D

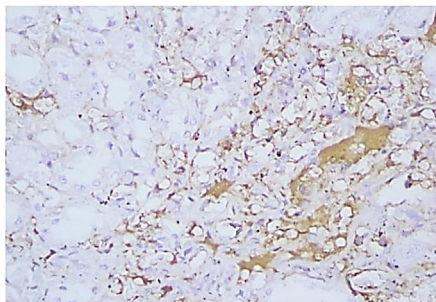


C. Control Group

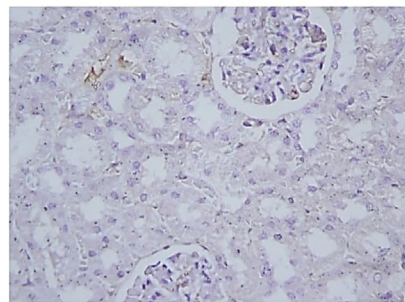


D. Necrostatin-1 Group

MLKL



E. Control Group



F. Necrostatin-1 Group

Fig 2. Immunohistochemical staining of apoptotic markers in experimental ischemic renal parenchymal tissue. **(A)** Caspase-3 staining showing increased apoptosis in the tubular epithelium in the control group ($\times 400$). **(B)** Significant reduction of apoptosis under the action of Necrostatin-1 ($\times 400$) (only a few cells show Caspase-3 staining). **(C)** Strong staining with gasdermin D in the control group ($\times 400$). **(D)** Positive effect of Necrostatin-1 on pyroptosis; gasdermin D staining is seen in a few tubular epithelium ($\times 400$). **(E)** Strong staining of MLKL, a marker of necroptosis, is seen in renal tubules ($\times 400$). **(F)** How much Necrostatin-1 reduces apoptotic cells remains to be seen. Necroptosis marker MLKL stained in only a few cells ($\times 400$). MLKL, Mixed Lineage Kinase Domain Like Pseudokinase.

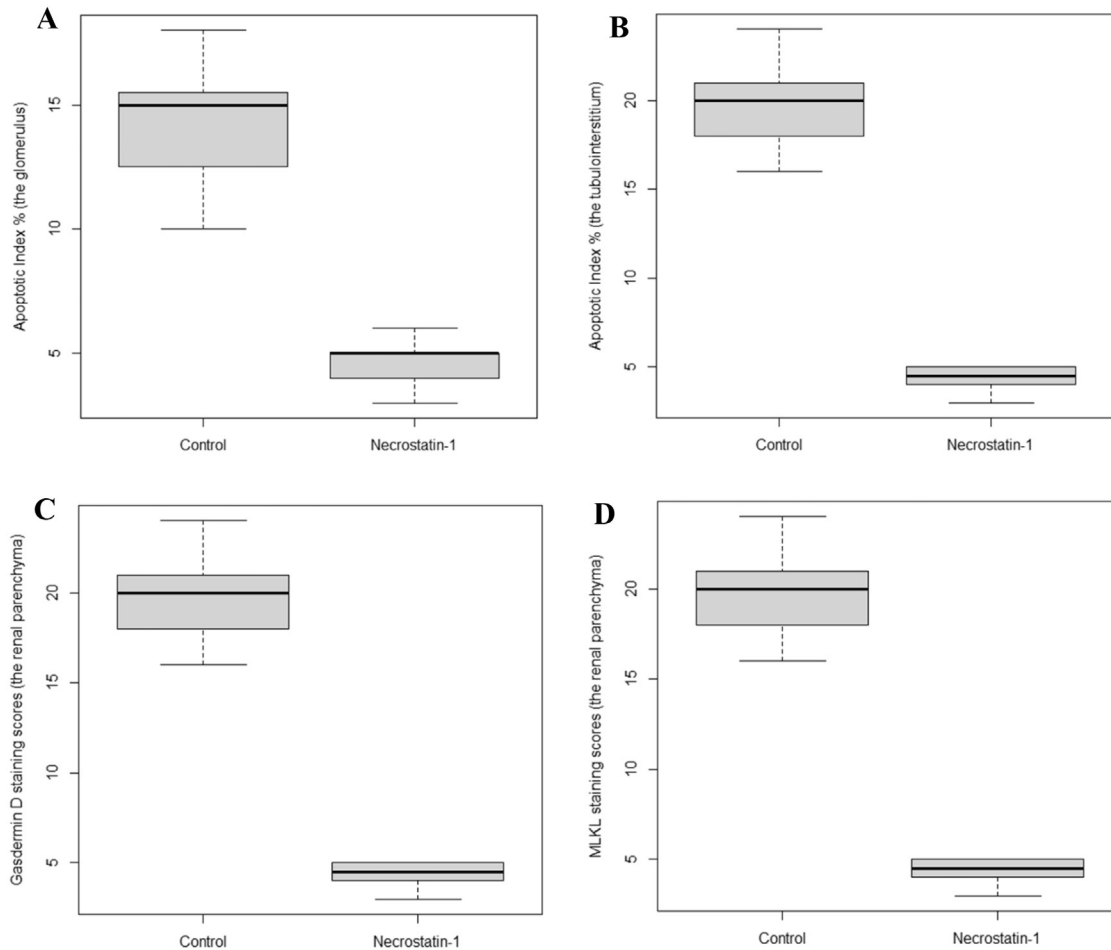


Fig 3. The distribution of the apoptotic index and staining scores of a proapoptotic marker Caspase-3, a proptosis mediator gasdermin D, and a necroptosis-related protein MLKL in ischemic renal tissue of a nonheart-beating donor model. **(A)** Apoptotic index distribution in the glomerulus. **(B)** Apoptotic index distribution in the renal tubulointerstitium. **(C)** Distribution of gasdermin D staining scores in the renal parenchyma. **(D)** Distribution of MLKL staining scores in the renal parenchyma. MLKL, Mixed Lineage Kinase Domain Like Pseudokinase.

significant. The amount of MDA in the Nec-1 group showed a significant reduction compared to the control group ($P = .009$). There was a slight drop in terms of 8-OH-dG amount in the experimental group compared to the control group, but like in CAT activity, the difference was not significant ($P = .20$) (Table 2).

DISCUSSION

Donors after circulatory death (DCD) is a crucial component of kidney transplantation. DCD renal transplantation is associated with a higher risk of complications, such as DGF, primary graft nonfunction, or acute rejection. These complications have an impact on both short- and long-term graft function and survival, thereby restricting the use of DCD. Nonheart-beating time may lead to inadequate renal perfusion, resulting in thermal ischemia of the kidney, clinically manifesting as DGF or primary graft nonfunction [30–33]. Our experimental rat study demonstrates

that Nec-1 effectively protects against RIR by inhibiting necroptosis, oxidative stress, and inflammation, as evidenced by histopathological and tissue-level biochemical findings. Nec-1, which reduces apoptosis, and pyroptosis, as well as the expression of proteins involved in all three pathways. MLKL is a pro-necroptotic protein that necrosomes turn on. During the reduced necroptosis process, Complex IIc will not be able to form. This means that MLKL will not be able to phosphorylate or become active. This will also lead to a reduction in its protein expression. It is known that necrostatin-1 (Nec-1) suppresses the synthesis of many pyroptosis mediators; a low Gasdermin D level is not an unexpected result and is compatible with the literature [6–8]. Nec-1 also inhibits gasdermin D activation by weakening the caspase-1 cascade via RIPK1 and ZBP1 [9,34,35]. This study involved creating an NHBD rat model through experiments, and the results indicated that administering Nec-1 before a cardiac arrest can decrease pyroptosis, apoptosis, and necroptosis. There was less tubular damage, glomerular and tubular

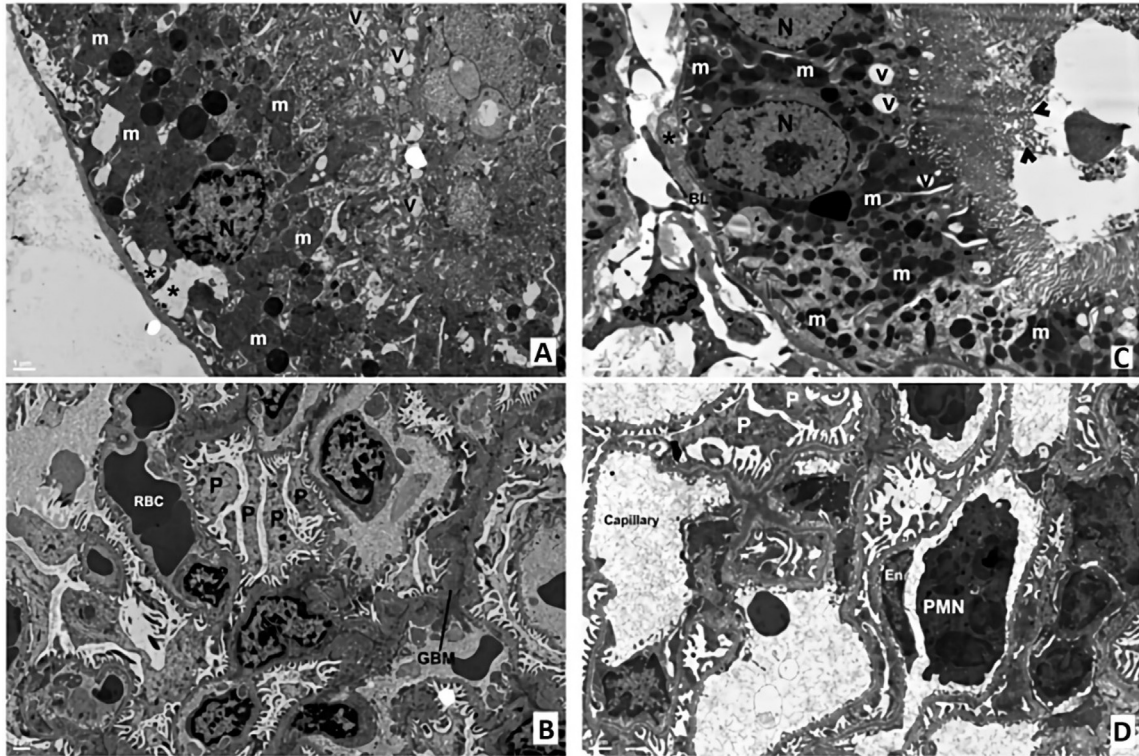


Fig 4. Representative transmission electron micrographs of the control group (**A** and **B**) and the Necrostatin-1 group (**C** and **D**). (**A**) The prominent edematous areas (*) and vacuoles (V) in cytoplasm, nuclear (N) chromatin irregularities, and loss of electron density of mitochondria (m) are remarkable in proximal tubule cells (Bar: 1 m). (**B**) Podocytes are seen with their foot processes in normal fine structure (Bar: 1 m). GBM, glomerular basement membrane; RBC, red blood cell. (**C**) Vacuoles (V), mitochondria (m) in cytoplasm, and microvilli hypertrophy (arrowheads) at the apical surface of the proximal tubule cell are observed; Lamination (*) in the basal lamina (BL) is noteworthy (Bar: 1 m). (**D**) Glomerulus showed normal fine structure as well as typical endothelial cells (En) and podocytes (P); Polymorphonuclear neutrophilic granulocytes (PMN) can be detected in the capillary lumen (Bar: 1 m).

API, gasdermin D, and MLKL in the group that got Nec-1 compared to the control group. Additionally, free oxygen radicals decreased, and the antioxidant defense system increased in the Nec-1 group. More electron microscopy results showed that the kidneys looked better at the ultrastructural level and that necroptotic renal cell death had gotten better. In addition to fixing problems like intracellular edema, vacuoles, and basal lamina rupture in renal tubular cells, nectin also made them better.

Table 2. Alteration of Oxidative Stress Markers After Renal Ischemic Injury

Markers	Group 1 (Control) (n = 12)	Group 2 (Nec-1) (n = 12)	P*
SOD (U/mg prt)	4.2 ± 2.3	6.9 ± 3.9	.007
GPx (U/mg prt)	0.26 ± 0.08	0.49 ± 0.22	.006
CAT (U/mg prt)	4588 ± 1916	4680 ± 1451	.47
MDA (nmol/mg prt)	8.8 ± 1.2	7.5 ± 1.1	.009
8-OH-dG (ng/mg of DNA)	2.5 ± 2.1	1.4 ± 0.8	.20

8-OH-dG, 8-Okso-2'-deoksiguanozin; CAT, catalase; GPx, glutathione peroxidase; MDA, malondialdehyde; Nec-1, Necrostatin-1; SOD, superoxide dismutase.

* P-values obtained from nonparametric Wilcoxon tests.

Researchers found that Nec-1 protects the kidney in the NHBD model of ischemic acute kidney injury by selectively suppressing RIPK1, a PANoptosome protein, to decrease PANoptosis [7,8]. Recently, researchers identified the PANoptosome, a cytoplasmic protein complex, as a new method of proinflammatory-programmed cell death that simultaneously triggers pyroptosis, apoptosis, and necroptosis [34,35]. These three types of planned cell death are very important in the complicated processes that lead to RIRI. Previous studies have shown that targeting pyroptosis, apoptosis, and necroptosis individually can protect against RIRI [36]. But because the PANoptosome controls all three types of programmed cell death, blocking certain PANoptosome proteins could stop the pathway that connects them and stop pyroptosis, apoptosis, and necroptosis all at the same time. Because of this, in this study, we used Nec-1, a specific inhibitor of RIPK1, to target and stop RIPK1, one of the PANoptosome proteins [9]. Previous studies have shown that Nec-1 can protect the kidney against RIRI by reducing necrosis and inflammation. Besides, Nec-1 is effective in blocking necroptosis by inhibiting RIPK1 [34,37]. This study observed changes induced by renal ischemia using the NHBD model but did not study changes during reperfusion. Therefore, it is crucial

to choose an agent that can effectively safeguard against acute ischemia and injury to the kidneys. This is especially important because necrosis, oxidative stress, and inflammation play such important roles in the pathophysiology of acute ischemic renal damage. Apoptosis is a mode of programmed cell death, and it also has a crucial function in RIRI [35]. Caspase activation is crucial in complex apoptotic pathways, with Caspase-3 playing a critical role in the apoptosis execution phase. During apoptosis, the renal tubules release proinflammatory cytokines that aid in cell death. Caspases activate in response to the release of inflammatory cytokines [34]. Caspase-3 is an apoptotic marker in PANoptosome, and we measured the API using Caspase-3 expression [38]. This study revealed lower Caspase-3 activity in the experimental group, as increased apoptosis can cause tissue damage. Wang et al [30] and Shan et al [39] found that nicotiflorin and allicin could protect kidneys from RIRI by lowering caspase-3 levels and cell death. Another study, using an extrarenal ischemia-reperfusion model, also found that organ protection was associated with a reduction in apoptosis and caspase-3 values [37,40]. Uysal et al [20] also showed that milrinone protects the kidney by lowering the levels of caspase-3 and the API in the NHBD model. Previous studies have demonstrated that renal ischemia causes apoptosis in all kidney tissue [34]. Our results confirm the previous findings, demonstrating a decrease in the API of both tubular and glomerular cells in the experimental group.

Pyroptosis is another important mode of programmed cell lysis. Pyroptosis, mainly occurring upon infection with intracellular pathogens, is a highly inflammatory process that has also been associated with RIRI [41]. Gasdermin D, a cytoplasmic protein, is crucial for triggering pyroptosis, and the release of interleukin-1 is also responsible for pyroptosis. In addition, nearly all gasdermins share the pore-forming and pyroptotic activity of gasdermin D [42]. This study demonstrated a significant decrease in gasdermin D expression in the Nec-1 group. Given that a lower level of gasdermin D correlates with less inflammatory cytokine release and pyroptosis, our findings suggest that Nec-1 may mitigate the damage that pyroptosis causes to cells and tissues. Previous reports have reported a protective effect of pyroptosis reduction against myocardial, cerebral, and kidney cell damage. [7,36,43] Microbial infections, on the other hand, have pathogenic triggers [44]. According to Miao et al [45], gasdermin-dependent pyroptosis of renal tubule cells is an important process in the onset of tubular cell destruction. Also, Pang et al [37] said that stopping pyroptosis linked to caspase-1 in mice that were given salvianolic acid B protects against kidney RIRI by turning on the Nrf2/NLRP3 signaling pathway. Also, Chueh et al [46] said that inhibiting thromboxane A2 synthase activities and activating the thromboxane prostanoid binding site protects the kidney from RIRI by lowering interleukin-1, gasdermin D, caspase-1, and pyroptosis. Taking all of this into account, our findings on gasdermin D and pyroptosis are consistent with previous studies.

Another type of programmed cell death associated with inflammation is necroptosis [47]. Previous studies have stressed that necroptosis is one of the responsible mechanisms for RIRI and tried to modulate necroptosis to diminish RIRI. Researchers

have linked necroptosis to the pathogenesis of oxidative stress and inflammation in ischemic acute kidney injury [6,7]. Several proteins, including RIPK1, RIPK-3, and MLKL, regulate necroptosis, and RIPK-3-mediated phosphorylation of MLKL drives it [48]. These proteins are considered necroptotic markers, with MLKL being a critical effector molecule. There have also been reports of (RIPK1) acting as a regulator for RIRI [7,8,33,35]. The association between RIPK3- and MLKL-dependent necroptosis and early RIRI Chen et al [49] demonstrated that inhibition of primary necroptotic pathway components, like MLKL, RIPK1, and RIPK-3, minimizes RIRI. Moreover, they concluded that necroptosis activated the NLRP3 inflammasome. Liao et al [50] did another study that showed how MLKL, (RIPK1), and RIPK3 were linked to renal necroptosis. They found that MLKL, (RIPK1), and RIPK3 levels rose during renal ischemia and decreased during both hypoxia and reoxygenation. Thus, they highlighted the importance of protecting the kidney against RIRI by regulating necroptosis in the RIP1/RIP3/MLKL pathway. Besides, they demonstrated that Nec-1 is protective against RIRI by reducing MLKL expression. The authors assert that the development of acute renal failure hinges on necroptosis in proximal tubules, a process that protects kidney tubular cells by inhibiting MLKL and reducing necroptosis. Finally, Martens et al [51] said that sorafenib tosylate lowers MLKL levels by stopping RIPK1 and RIPK3. Because it stops tumor necrosis factor-linked necroptosis, they were able to show that this drug was good for the kidney tissue in RIRI by lowering MLKL expression and necroptosis. In our study, we used Nec-1 to examine the expression of MLKL, the necroptosis marker. Our findings showed that MLKL expression decreased in the Nec-1 group. Low MLKL is linked to decreased necroptosis. Our results support the findings of the previous studies. During renal ischemia, increasing free oxygen radical levels leads to cellular damage. Particularly, lipid peroxidation by free oxygen radicals aggravates kidney injury, and reperfusion causes additional tissue damage [52]. Antioxidant enzymes like GPx, SOD, and CAT exert protective functions against free oxygen radical damage. Fatty acid peroxidation causes the cell to produce MDA. As the number of free oxygen radicals increases, MDA production also increases. Increased MDA production indicates elevated oxidative stress [4–6]. In their study on RIRI, Shen et al [31] looked at oxidative stress in rats by measuring MDA and the NADP+/NADPH ratio. They found that the ratio of MDA and NADP+/NADPH decreased significantly in rats administered Nec-1. In another recent study, Li et al [53] found a significant reduction in RIRI in rats administered hydralazine. They found that the hydralazine-treated group had higher CAT, SOD, and GSH-Px levels, but MDA levels were much lower. They then concluded that the increased activity of the antioxidant defense system reduces kidney damage. Similarly, in this study, we observed that the MDA level considerably diminished in the treated group. Therefore, we may link the Nec-1 Group's low MDA level to lower oxidative stress. Although SODs and GPx activities alone do not reflect the cellular redox state, they are crucial enzymes that aid in understanding the level of oxidative stress and directly contribute to the process. Given that GPx

always needs reduced glutathione (GSH) to work, higher GPx activity also means that the cellular GSH/GSSG ratio is higher. While numerous parameters exist for measuring oxidative stress and cellular redox status, study limitations necessitate the selection of a select few [54]. In this study, we chose three important antioxidant enzymes, SOD, CAT, and GPX, to evaluate their antioxidant potential. To evaluate oxidative damage, we chose MDA as an indicator of lipid peroxidation and 8-oxodG as an indicator of DNA oxidation. It is not currently possible to determine how much of 8-oxodG comes from damaged cells and how much from dead cells. However, the 8-oxodG level we measured is an important and specific parameter because it shows the total level of all dead and severely damaged cells damaged at the DNA level, as well as the severity of oxidative damage [55]. It is widely accepted that antioxidants, like GSH-Px, CAT, and SOD, are protective for the kidney in the course of RIRI. SOD, CAT, and GSH-Px levels drop drastically during RIRI, whereas free oxygen radicals rise. Free oxygen radicals can lessen cell and tissue damage by raising CAT, SOD, and GSH-Px levels [56]. In this study, we aimed to reveal to what extent reagent production and oxidative damage occur by measuring lipid peroxidation. The study's scope was not to investigate the effect of lipid peroxides on the PANOptosis process and mechanism. In a separate study, we aim to investigate the effects of intracellular oxidation products formed as a result of oxidative damage on the PANOptosis process. We will try to implement your valuable suggestion in our study. Although there is a strong relationship between pyroptosis, apoptosis, and lipid peroxidation, inhibition of lipid peroxidation plays a major role in reducing tissue damage for antioxidant defense systems [7–9,34]. Moreover, iron overload, glutathione depletion, and a buildup of lipid peroxides control ferroptosis, a recently discovered type of cell death [57]. Recent scientific evidence has shown that ferroptosis is implicated in acute kidney injury generated by ischemia or reperfusion and plays a pivotal role in the demise of renal tubular cells [58]. Given that synthetic forms of cell death pathways can cause renal damage, and that our experimental study used Nec-1, a classical inhibitor for necroptosis, will inhibitors for other cell death pathways have the same protective effect? Different antioxidants, like ferrostatin-1 and liproxstatin-1, which stop lipid peroxidation, and the apoptosis inhibitor Q-VD-Oph, may work in a similar way to protect cells [59]. Experimental research using new apoptosis inhibitors is required to address all these questions. The results of this study were consistent with previous studies in that the rats treated with Nec-1 had significantly increased levels of SOD and GSH-Px. Nec-1 administration also augmented CAT levels, although the difference between the groups was not significant. Therefore, we may link lower oxidative stress to higher amounts of GSH-Px, SOD, and CAT. Other research also suggests that boosting these antioxidant defense systems can reduce oxygen radical-induced cell damage [10–12,15,34,54]. In light of the above current literature information on Nec-1, we can say that inhibition of RIP1-mediated necroptosis, also referred to as caspase-independent cell death, through the use of Nec-1 or the highly specific RIP1 inhibitor provides protection against RIRI. Linkermann et al [60] carried out an experimental study on rats, demonstrating that Nec-1 treatment decreased organ damage and renal failure, even when

administered after reperfusion, resulting in a significant survival advantages in a model of lethal RIRI. This finding is based on the decrease of histological and ultrastructural issues affecting ischemia renal tissue in NHBD rat groups administered Nec-1 prior to circulatory death, as well as the diminution of elevated ROS levels during the RIRI process. A summary of current study results and experimental studies on the effects of Nec-1 on ischemic processes reveals that it is effective when provided both before and after RIRI in renal transplant surgery. In this context, this experimental rat study specifically indicates Nec-1's potential as a healing agent that provides effective nephroprotection during early warm ischemia in renal transplant patients.

In conclusion, this experimental animal study demonstrated that administering Nec-1 to NHBD rats prior to DCD markedly reduced renal tubular injury, the API of glomeruli and tubules, and the expressions of gasdermin D and MLKL in their ischemic renal tissue. It also shown that Nec-1 significantly decreased ROS levels in renal tissue during ischemia and subsequently stimulated the antioxidant defense mechanism. Furthermore, our immunohistochemical and electron microscopic analyses indicated that the ischemia-sensitive renal tissues of rats treated with Nec-1 exhibited sign of necroptosis including intracellular edema, vacuolation, and basal lamina rupture, at a slower and less severe rate. In contrast, rats that were not given Nec-1 had a more rapid rate of kidney cell degradation. Our findings indicate that Nec-1 can effectively protect against RIRI by inhibiting necroptosis, oxidative stress, and inflammation. Hence, administration of Nec-1 during early warm ischemia period can alleviate cell death and improve the cell viability of tubules and interstitial tissue in NHBDs with determined circulatory death. Regardless of its RIP1-independent inhibitory effects, metabolic instability, and off-target effects that restrict its usage and nephroprotective efficacy following RIRI, Nec-1 might offer novel opportunities for protecting the donor kidney from RIRI in patients for kidney transplantation.

Limitations

An important limitation of this experimental study lies in its focus on ROS and antioxidant activity in ischemic renal tissues during the warm ischemic phase. It only examines the short-term histopathological, immunohistochemical, and electron microscopic changes in the renal tubules and interstitium following renal ischemia in NHBD rats after circulatory death. However, it lacks a transplant ischemia-reperfusion step. Currently, it remains uncertain whether the effects of Nec-1 on ischemic injury will persist after perfusion and/or significantly impact organ function in a recipient. This research will need to be supported by longer, prospective new experimental studies focusing on renal function, including the renal transplant ischemia-reperfusion step.

FUNDING

The author declared that this study has received no financial support.

DATA AVAILABILITY

Data will be made available on request.

DECLARATION OF COMPETING INTEREST

None declared.

ACKNOWLEDGMENTS

We would like to thank the staff of the Experimental Animal Laboratory of Kahramanmaraş Sutcu Imam University Faculty of Medicine and also Assoc. Prof. Dr Nadire Eser PhD from the Department of Medical Pharmacology for their support in carrying out this experimental study.

REFERENCES

- [1] Yıldız I, Koca YS, Sabuncuoğlu MZ. Urgent organ retrieval from non-heart-beating donor with declared brain death: harvest at arrest. *Chirurgia (Bucur)* 2017;112:130–5.
- [2] Nishikido M, Noguchi M, Koga S, et al. Kidney transplantation from non-heart-beating donors: analysis of organ procurement and outcome. *Transplant Proc* 2004;36:1888–90.
- [3] Teraoka S, Nomoto K, Kikuchi K, et al. Outcomes of kidney transplants from non-heart-beating deceased donors as reported to the Japan Organ Transplant Network from April 1995–December 2003: a multi-center report. *Clin Transpl* 2004;91–102.
- [4] Treska V, Kober J, Hasman D, et al. Ischemia-reperfusion injury in kidney transplantation from non-heart-beating donor—do antioxidants or antiinflammatory drugs play any role? *Bratisl Lek Listy* 2009;110:133–6.
- [5] Gholampour H, Moezi L, Shafaroodi H. Aripiprazole prevents renal ischemia/reperfusion injury in rats, probably through nitric oxide involvement. *Eur J Pharmacol* 2017;813:17–23.
- [6] Shi C, Cao P, Wang Y, et al. PANoptosis: a cell death characterized by pyroptosis, apoptosis, and necroptosis. *J Inflamm Res* 2023;16:1523–32.
- [7] Dugbartey GJ. Cellular and molecular mechanisms of cell damage and cell death in ischemia-reperfusion injury in organ transplantation. *Mol Biol Rep* 2024;51:473.
- [8] Choudhury SM, Sarkar R, Karki R, Kanneganti TD. A comparative study of apoptosis, pyroptosis, necroptosis, and PANoptosis components in mouse and human cells. *PLoS One* 2024;19:e0299577.
- [9] Samir P, Malireddi RKS, Kanneganti TD. The PANoptosome: a deadly protein complex driving pyroptosis, apoptosis, and necroptosis (PANoptosis). *Front Cell Infect Microbiol* 2020;10:238.
- [10] Xie J, Guo Q. Apoptosis antagonizing transcription factor protects renal tubule cells against oxidative damage and apoptosis induced by ischemia-reperfusion. *J Am Soc Nephrol* 2006;17:3336–46.
- [11] Sun X, Yang Y, Meng X, Li J, Liu X, Liu H. PANoptosis: mechanisms, biology, and role in disease. *Immunol Rev* 2024;321:246–62.
- [12] Cai Y, Xiao H, Zhou Q, et al. Comprehensive analyses of PANoptosome with potential implications in cancer prognosis and immunotherapy. *Biochem Genet* 2024. doi: 10.1007/s10528-024-10687-8.
- [13] Ashour H, Hashem HA, Khowailed AA, Rashed LA, Hassan RM, Soliman AS. Necrostatin-1 mitigates renal ischaemia-reperfusion injury—time dependent—via aborting the interacting protein kinase (RIPK-1)-induced inflammatory immune response. *Clin Exp Pharmacol Physiol* 2022;49:501–14.
- [14] Cao L, Mu W. Necrostatin-1 and necroptosis inhibition: pathophysiology and therapeutic implications. *Pharmacol Res* 2021;163:105297.
- [15] Hu QH, Luo FY, Luo WJ, Wang L. Ischemic postconditioning reduces ischemic reperfusion injury of non-heart-beating donor grafts in a rat lung transplant. *Exp Clin Transplant* 2013;11:44–9.
- [16] Niu X, Huang WH, De Boer B, Delriviere L, Mou LJ, Jeffrey GP. Iron-induced oxidative rat liver injury after non-heart-beating warm ischemia is mediated by tumor necrosis factor α and prevented by deferoxamine. *Liver Transpl* 2014;20:904–11.
- [17] AVMA guidelines for the euthanasia of animals: 2013 edition members of the panel on euthanasia. Available at https://www.academia.edu/30520069/AVMA_Guidelines_for_the_Euthanasia_of_Animals_2013_Edition_Members_of_the_Panel_on_Euthanasia [Accessed 3 April 2024].
- [18] Alghannam K, Howard B, Loza J, et al. A survey of united states transplant center donation after circulatory death kidney transplant practices in the modern era. *Transplant Proc* 2024;56:1712–20.
- [19] Laskowski IA, Pratschke J, Wilhelm MM, et al. Early and late injury to renal transplants from non-heart-beating donors. *Transplantation* 2002;73:1468–73.
- [20] Uysal E, Dokur M, Altınay S, et al. Investigation of the effect of milrinone on renal damage in an experimental non-heart beating donor model. *J Invest Surg* 2018;31:402–11.
- [21] Hsu SM, Raine L, Fanger H. The use of antiavidin antibody and avidin-biotin-peroxidase complex in immunoperoxidase technics. *Am J Clin Pathol* 1981;75:816–21.
- [22] Bradford MM. A rapid and sensitive method for the quantitation of microgram quantities of protein utilizing the principle of protein-dye binding. *Anal Biochem* 1976;72:248–54.
- [23] Mihara M, Uchiyama M. Determination of malondialdehyde precursor in tissues by thiobarbituric acid test. *Anal Biochem* 1978;86:271–8.
- [24] McCord JM, Fridovich I. Superoxide dismutase. An enzymic function for erythrocyte (hemocuprein). *J Biol Chem* 1969;244:6049–55.
- [25] Aebi H. Catalase. In: Bergmeyer HU, editor. *Methods of enzymatic analysis*. Weinheim/New York: Verlag Chemie/Academic Press Inc; 1974. p. 673–80.
- [26] Lawrence RA, Burk RF. Glutathione peroxidase activity in selenium-deficient rat liver. *Biochem Biophys Res Commun* 1976;71:952–8.
- [27] Gupta RC. 32P-postlabelling analysis of bulky aromatic adducts. *IARC Sci Publ* 1993(124):11–23.
- [28] Shibayama S, Fujii SI, Inagaki K, Yamazaki T, Takatsu A. Formic acid hydrolysis/liquid chromatography isotope dilution mass spectrometry: an accurate method for large DNA quantification. *J Chromatogr A* 2016;1468:109–15.
- [29] Chen CY, Zhou YT, Lee HL, Lin YW. Simultaneous, rapid, and sensitive quantification of 8-hydroxy-2'-deoxyguanosine and cotinine in human urine by on-line solid-phase extraction LC-MS/MS: correlation with tobacco exposure biomarkers NNAL. *Anal Bioanal Chem* 2016;408:6295–306.
- [30] Wang L, Li C, Guan C, et al. Nicotiflorin attenuates cell apoptosis in renal ischemia-reperfusion injury through activating transcription factor 3. *Nephrology (Carlton)* 2021;26:358–68.
- [31] Shen B, Mei M, Pu Y, et al. Necrostatin-1 attenuates renal ischemia and reperfusion injury via mediation of HIF-1 α /mir-26a/TRPC6/PARP1 signaling. *Mol Ther Nucleic Acids* 2019;17:701–13.
- [32] Dong L, Liang F, Lou Z, et al. Necrostatin-1 alleviates lung ischemia-reperfusion injury via inhibiting necroptosis and apoptosis of lung epithelial cells. *Cells* 2022;11:3139.
- [33] Cao Y, Wang HB, Ni CJ, Chen SL, Wang WT, Wang LR. Necrostatin-1 prevents skeletal muscle ischemia reperfusion injury by regulating Bok-mediated apoptosis. *J Chin Med Assoc* 2023;86:26–33.
- [34] Christgen S, Zheng M, Kesavardhana S, et al. Identification of the PANoptosome: a molecular platform triggering pyroptosis, apoptosis, and necroptosis (PANoptosis). *Front Cell Infect Microbiol* 2020;10:237.
- [35] Jun W, Benjanuwattra J, Chattipakorn SC, Chattipakorn N. Necroptosis in renal ischemia/reperfusion injury: a major mode of cell death? *Arch Biochem Biophys* 2020;689:108433.

- [36] Pandian N, Kanneganti TD. PANoptosis: a unique innate immune inflammatory cell death modality. *J Immunol* 2022;209:1625–33.
- [37] Pang Y, Zhang PC, Lu RR, et al. Andrade-Oliveira salvianolic acid B modulates caspase-1-mediated pyroptosis in renal ischemia-reperfusion injury via Nrf2 pathway. *Front Pharmacol* 2020;11:541426.
- [38] Perry DK, Smyth MJ, Stennicke HR, et al. Zinc is a potent inhibitor of the apoptotic protease, caspase-3. A novel target for zinc in the inhibition of apoptosis. *J Biol Chem* 1997;272:18530–3.
- [39] Shan Y, Chen D, Hu B, et al. Allicin ameliorates renal ischemia/reperfusion injury via inhibition of oxidative stress and inflammation in rats. *Biomed Pharmacother* 2021;142:112077.
- [40] Karimi Z, SoukhakLari R, Rahimi-Jaberi K, Esmaili Z, Moosavi M. Nanomicellar curcuminoids attenuates renal ischemia/reperfusion injury in rat through prevention of apoptosis and downregulation of MAPKs pathways. *Mol Biol Rep* 2021;48:1735–43.
- [41] Yang JR, Yao FH, Zhang JG, et al. Ischemia-reperfusion induces renal tubule pyroptosis via the CHOP-caspase-11 pathway. *Am J Physiol Renal Physiol* 2014;306:F75–84.
- [42] Liu X, Zhang Z, Ruan J, et al. Inflammasome-activated gasdermin D causes pyroptosis by forming membrane pores. *Nature* 2016;535:153–8.
- [43] Zhang J, Huang L, Shi X, et al. Metformin protects against myocardial ischemia-reperfusion injury and cell pyroptosis via AMPK/NLRP3 inflammasome pathway. *Aging (Albany NY)* 2020;12:24270–87.
- [44] Place DE, Lee S, Kanneganti TD. PANoptosis in microbial infection. *Curr Opin Microbiol* 2021;59:42–9.
- [45] Miao N, Yin F, Xie H, et al. The cleavage of gasdermin D by caspase-11 promotes tubular epithelial cell pyroptosis and urinary IL-18 excretion in acute kidney injury. *Kidney Int* 2019;96:1105–20.
- [46] Chueh TH, Cheng YH, Chen KH, Chien CT. Thromboxane A2 synthase and thromboxane receptor deletion reduces ischaemia/reperfusion-evoked inflammation, apoptosis, autophagy and pyroptosis. *Thromb Haemost* 2020;120:329–43.
- [47] Li X, Ling Y, Cao Z, et al. Targeting intestinal epithelial cell-programmed necrosis alleviates tissue injury after intestinal ischemia/reperfusion in rats. *J Surg Res* 2018;225:108–17.
- [48] Liu W, Chen B, Wang Y, et al. RGMb protects against acute kidney injury by inhibiting tubular cell necroptosis via an MLKL-dependent mechanism. *Proc Natl Acad Sci USA* 2018;115:E1475–84.
- [49] Chen H, Fang Y, Wu J, et al. RIPK3-MLKL-mediated necroinflammation contributes to AKI progression to CKD. *Cell Death Dis* 2018;9:878.
- [50] Liao YJ, Ma YX, Huang LL, et al. Augmenter of liver regeneration protects the kidney against ischemia-reperfusion injury by inhibiting necroptosis. *Bioengineered* 2022;13:5152–67.
- [51] Martens S, Jeong M, Tonnus W, et al. Sorafenib tosylate inhibits directly necrosome complex formation and protects in mouse models of inflammation and tissue injury. *Cell Death Dis* 2017;8:e2904.
- [52] Yun Y, Duan WG, Chen P, et al. Ischemic postconditioning modified renal oxidative stress and lipid peroxidation caused by ischemic reperfusion injury in rats. *Transplant Proc* 2009;41:3597–602.
- [53] Li Y, Hou D, Chen X, et al. Hydralazine protects against renal ischemia-reperfusion injury in rats. *Eur J Pharmacol* 2019;843:199–209.
- [54] Alaaeldin R, Bakkar SM, Mohyeldin RH, Ali FEM, Abdel-Maqsood NMR, Fathy M. Azilsartan modulates HMGB1/NF- κ B/p38/ERK1/2/JNK and apoptosis pathways during renal ischemia reperfusion injury. *Cells* 2023;12:185.
- [55] Kuroda K, Ishii Y, Takasu S, et al. Possible contribution of 8-hydroxydeoxyguanosine to gene mutations in the kidney DNA of GPT delta rats following potassium bromate treatment. *Mutat Res Genet Toxicol Environ Mutagen* 2024;894:503729.
- [56] Bircan B, Çakır M, Kırbağ S, Gül HF. Effect of apelin hormone on renal ischemia/reperfusion induced oxidative damage in rats. *Ren Fail* 2016;38:1122–8.
- [57] Su LJ, Zhang JH, Gomez H, et al. Reactive oxygen species-induced lipid peroxidation in apoptosis, autophagy, and ferroptosis. *Oxid Med Cell Longev* 2019;2019:5080843.
- [58] Shi Z, Du Y, Zheng J, et al. Liproxstatin-1 alleviated ischemia/reperfusion-induced acute kidney injury via inhibiting ferroptosis. *Antioxidants (Basel)* 2024;13:182.
- [59] Thapa K, Singh TG, Kaur A. Targeting ferroptosis in ischemia/reperfusion renal injury. *Naunyn Schmiedebergs Arch Pharmacol* 2022;395:1331–41.
- [60] Linkermann A, Bräsen JH, Himmerkus N, et al. Rip1 (receptor-interacting protein kinase 1) mediates necroptosis and contributes to renal ischemia/reperfusion injury. *Kidney Int* 2012;81:751–61.